

Real-Time Response and Phase-Sensitive Detection to Demonstrate the Validity of ESR-STM Results

Yishay Manassen

Department of Chemical Physics, The Weizmann Institute of Science, Rehovot 76100, Israel

Received October 18, 1996; revised February 25, 1997

In ESR-STM (1–3), the tip of a scanning tunneling microscope (STM) scans a surface which contains isolated paramagnetic spin centers. It was found previously that, in the presence of an external magnetic field, an AC component at the Larmor frequency appears in addition to the DC tunneling current and that this RF signal is spatially localized to a region with a radius of 0.5–1 nm. The AC signal was detected, after amplification, by a spectrum analyzer. An impedance-matching circuit is added to match the output impedance of the STM to 50 Ω and to optimize the sensitivity. The sample which was used for this observation was a silicon surface covered with several monolayers of SiO₂ produced by thermal oxidation, and the paramagnetic centers are isolated silicon dangling bonds located at the Si/SiO₂ interface (P_b centers).

Although it was shown that the signal observed was detected at the proper frequencies for different magnetic fields, this observation remained somewhat controversial. One claim was that there was no way of distinguishing between spurious signals which might accidentally exist at the frequency examined and the real signals. In this Note, this concern is eliminated by showing that the signals respond in real time to changes in the magnetic field: In addition to the static DC magnetic field, a small time-dependent sinusoidal field is applied. This field modulation causes a modulation of the signal. The response to the field modulation enables phase-sensitive detection (PSD). The previous observation of the two-dimensional spatial localization is reconfirmed; this time the signal is detected by PSD when the magnetic field is modulated. This observation eliminates concerns that the previous observations were due to traps or any other species on the surface which could, in principle, create a local increase in the high-frequency noise level.

Suppose that the signal is driven by a field (in frequency units) of the form $\omega_i = \omega_c + \Delta\omega \cos(\omega_m t)$, where ω_c is the carrier frequency, ω_m is the modulation frequency, and $\Delta\omega$ is the modulation intensity. This signal can be expressed as $F(t) = A \sin[\omega_c t + m_\omega \sin(\omega_m t)]$, where m_ω is the modulation index $m_\omega = \Delta\omega/\omega_m$. This is obtained by line integration

of ω_i to obtain the phase of the signal. Fourier expansion of this signal gives

$$F(t) = A \{ J_0(m_\omega) \sin(\omega_c t) + J_1(m_\omega) [\sin(\omega_c + \omega_m)t - \sin(\omega_c - \omega_m)t] + J_2(m_\omega) [\sin(\omega_c + 2\omega_m)t + \sin(\omega_c - 2\omega_m)t] + \dots \},$$

where $J_n(m_\omega)$ are n th-order Bessel functions of the first kind. For a large modulation index, there are many significant frequency terms. A spectral analysis results in a set of equally spaced sidebands, each separated by ω_m from a neighbor, and the sideband spectrum looks as in Fig. 1, bottom. The intensity of each sideband is given by J_n . The total number of sidebands of significant intensity in this spectrum is $2m_\omega$; they are too close to each other to be distinguished in Fig. 1. The frequency difference between the two largest sidebands at the two edges of this spectrum is approximately $2\Delta\omega$ (4).

In order to check the real-time response of ESR-STM signals, a coil was added to the STM that can generate a small oscillatory field component parallel to the DC magnetic field. Both fields are applied parallel to the tip. The DC magnetic field was 150.5 ± 0.5 G. The error of 0.5 G is due to the inhomogeneous component of the magnetic field which creates a slight variation in the intensity of the field. This occurs mainly because of small changes in the precise position of the tunneling region (for example, because of tips with different lengths). The precision of the gaussmeter is also ± 0.5 G. The modulation intensity ΔH was 27 mG. This was measured by applying a DC current to the coil and monitoring the change in the DC field. A change of the field by 2–3 G was measured. Then, by extrapolation, the field intensity for smaller current values was estimated. The error in the value of the modulation intensity is $\pm 10\%$. The modulation frequency was 300 Hz, the tunneling current was 1 nA, and the tip to sample bias voltage was 0.32 V. The static magnetic field, the tunneling current, and the tip to sample bias voltage were the same for all the measurements reported in this Note.

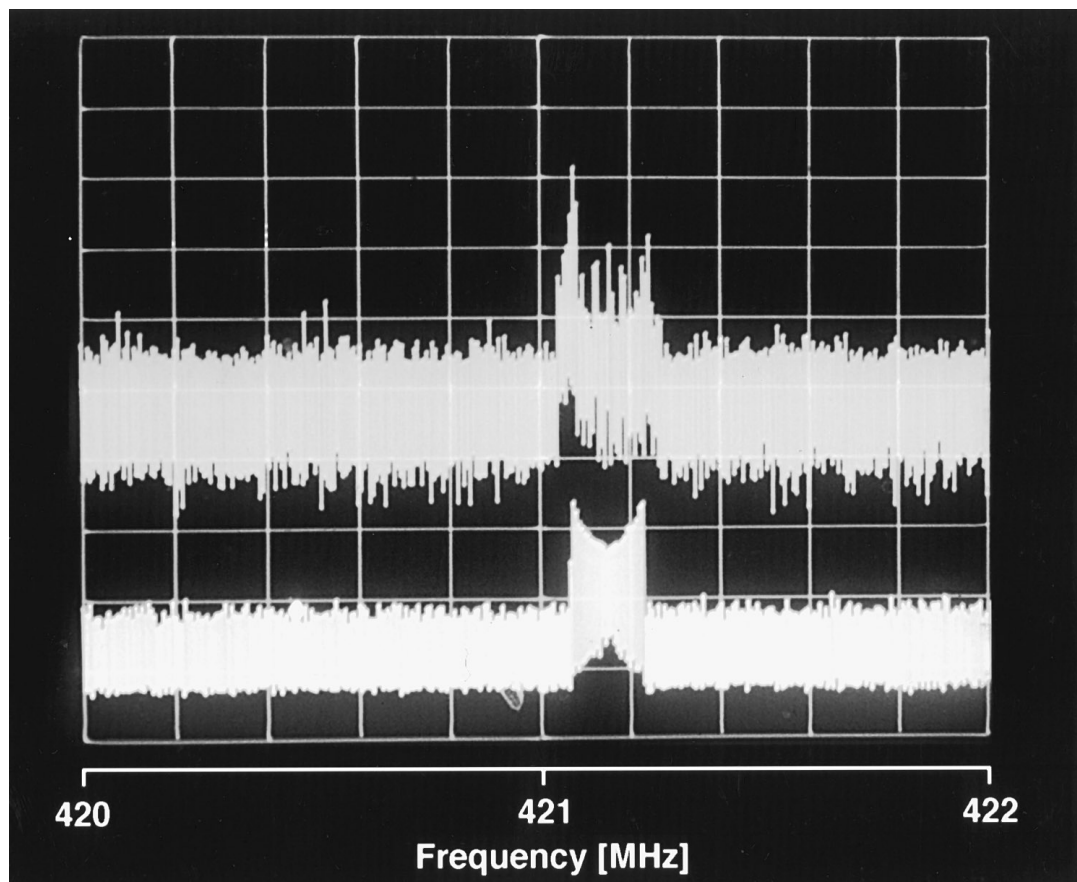


FIG. 1. (Top) A modulated ESR-STM signal detected only with a spectrum analyzer. It is observed under the conditions of field modulation described in the text. For comparison, an analogous frequency-modulated signal (bottom) from a frequency synthesizer is shown.

An ESR-STM signal observed in these circumstances is shown in Fig. 1, upper trace. For comparison, the lower trace shows a simulated frequency-modulated signal from a frequency synthesizer with the same modulation frequency and with modulation intensity of $\Delta\nu (= \Delta\omega/2\pi) = [g\beta\Delta H]/h = 75$ kHz ($m_\omega = 250$). The g value of the spin center is assumed to be 2. β is the Bohr magneton and h is Planck's constant. The similarity between the two traces is striking. Not only was the ESR-STM signal split with the frequency difference between the edges precisely $2\Delta\nu$, but even the lineshape is similar. This proves, beyond doubt, that the frequency of the signals depends, in real time, on the value of the magnetic field. No spurious signal known to the author can give such a response.

In order to achieve improved reliability, the real-time response of the ESR-STM signals was fed to a lock-in amplifier and a phase-sensitive signal was detected. However, since in this phase-sensitive detector the signal is mixed with a reference wave oscillating at $\nu_m (= \omega_m/2\pi)$, it is necessary to have a signal with a much smaller modulation index. To observe maximum sensitivity it is anticipated that m_ω should be close to 2, where the value of the J_1 term is the largest

and the intensity of the higher sidebands is negligible. Figure 2 provides a simple scheme of how such a phase-sensitive detector works in our system.

The spectrum analyzer works with a certain resolution bandwidth (marked in Fig. 2 by a rectangle). The phase of the output from the PSD depends on the relative frequency shift between the ESR-STM signal and the detection band of the spectrum analyzer. When the average frequency of the ESR-STM signal is smaller than the central frequency of the detection band, then the ν_m modulation will create a time-dependent output $S(t)$ in the spectrum analyzer which has the same phase as the reference wave and will give a positive output in the PSD (Figs. 2A and 2B). If the average frequency of the ESR-STM signal is higher than the central frequency of the detection band, the modulated output of the analyzer will be 180° out of phase with respect to the reference wave and will give a negative output in the PSD (Figs. 2C and 2D). Note that $S(t)$, the output of the spectrum analyzer, has only positive values due to the fact that it is an absolute-magnitude detector. For this reason when the lineshape of the unmodulated signal is perfectly symmetric, the lineshape observed at the PSD will look like the well-known symmetric derivative

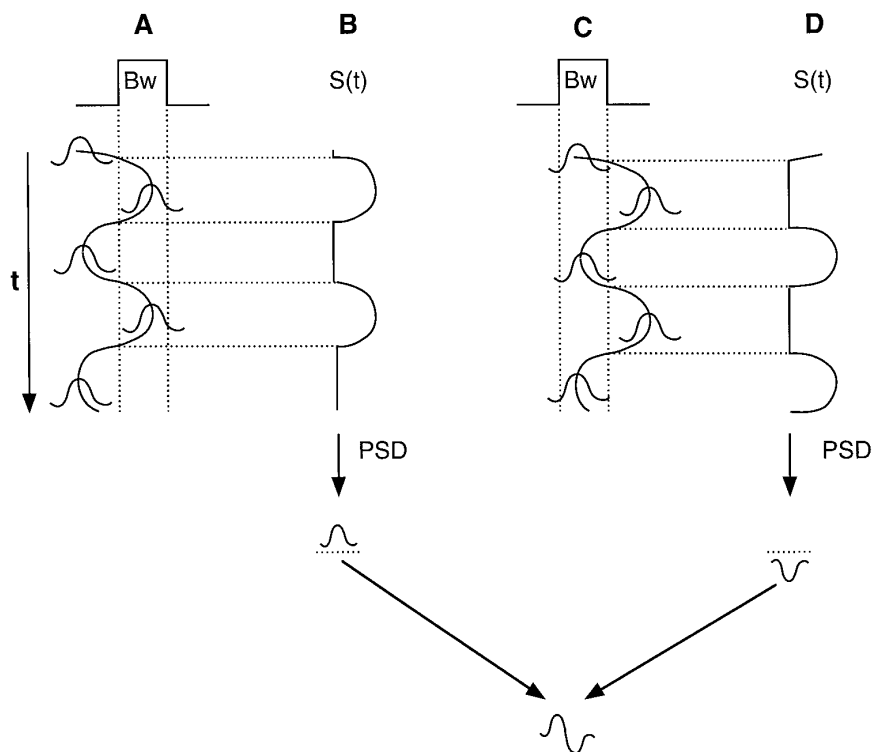


FIG. 2. A scheme of the detection mechanism with a spectrum analyzer and a lock-in amplifier. (A) The signal enters the detection band from the low-frequency side. (B) The relative phase between the output of the spectrum analyzer $S(t)$ and the field $H(t)$ creates a positive output at the PSD. (C) The signal enters the detection band from the high-frequency side. (D) This gives a negative output at the PSD. Altogether, this gives a derivative shape, as the spectrum analyzer sweeps the signal.

signal. This conclusion can be easily verified by detecting a synthesized frequency-modulated signal with a spectrum analyzer and a lock-in amplifier.

The main disadvantage of such a detection scheme is the fact that the sensitivity is a complex function of many parameters. In addition to the requirement that $m_\omega = 2$, $\Delta\nu$ should be of the same order of magnitude as the bandwidth of the spectrum analyzer. If $\Delta\nu$ is too small, there will be no modulation, since the modulated signal will stay within the detection band during the entire modulation cycle, and the output $S(t)$ of the spectrum analyzer will be time independent. On the other hand, if $\Delta\omega$ will be much larger than the bandwidth, the signal will be mostly out of the detection band during the modulation cycle, giving a weaker output $S(t)$. Additional important parameters are the sweep time of the analyzer, the time constant of the lock-in amplifier, and the phase of the lock-in amplifier. Fortunately, it is possible to search for the conditions of the optimal sensitivity with a synthesized signal. In such a simulation, however, the originally unmodulated signal is assumed to contain a single frequency ω_c . The effect of a finite linewidth of this signal on the observed sensitivity and lineshape in the phase-sensitive detector must be pronounced. Currently, however, we have no way of eliminating this spectral parameter from the observed PSD lineshapes.

Figure 3A shows a signal which has a derivative shape. This signal is detected under the conditions $\nu_m = 300$ Hz and $\Delta H = 20$ mG. This signal exhibits a good S/N ratio despite the large modulation index. C and E also have a similar derivative shape. However, B and D are examples of different lineshapes. These experiments were performed under variable conditions: B with $\nu_m = 20$ kHz and $\Delta H = 18$ mG; C, the same as B; D with $\nu_m = 3$ kHz and $\Delta H = 12.5$ mG; E, the same as D. Moreover, E was observed immediately after D without moving the tip. The signals shown in D and E originate from precisely the same region on the surface. Still, their lineshapes are different.

The phase-randomization phenomenon can be explained to some extent by small random fluctuations in the frequency and the lineshape of the ESR-STM signal. Asymmetric lineshapes of the ESR-STM signals are often observed. For example, in Fig. 1, top, the asymmetric shape of the modulated signal originates from an asymmetric shape of the unmodulated ESR-STM signal. This conclusion was verified with a simple computer simulation. However, in order to provide a complete explanation, one must gain a better understanding of the dynamics of the system, together with the mechanism by which the tunneling process is affected.

Two-dimensional spatial localization was demonstrated also for the modulated signal. Figure 4A shows a signal that

was detected by the two consecutive frequency sensors: the spectrum analyzer with a fixed frequency and a fixed bandwidth and the lock-in amplifier. Here, the spectrum analyzer works as a superheterodyne receiver. The experimental conditions were as follows: 421.7 MHz detection frequency, 300 kHz spectrum analyzer bandwidth, $\nu_m = 20$ kHz, and $\Delta H = 14$ mG. The phase of the signal fluctuates while the tip is scanning the region from which the signal originates. The fluctuations could be a measure of the small fluctuations in frequency of the ESR-STM signals. A signal with a fixed frequency should give either a positive or a negative output at the PSD depending on the relevant frequency shift be-

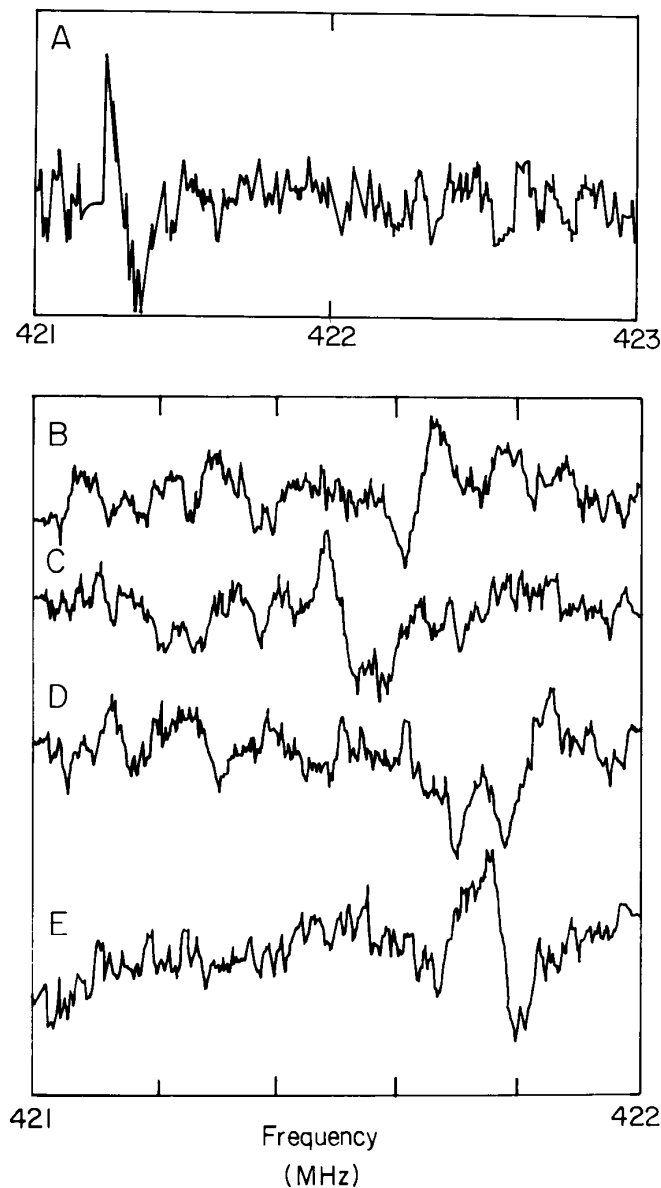


FIG. 3. Different ESR-STM spectra detected with a spectrum analyzer and a lock-in amplifier. The experimental modulation conditions are described in the text.

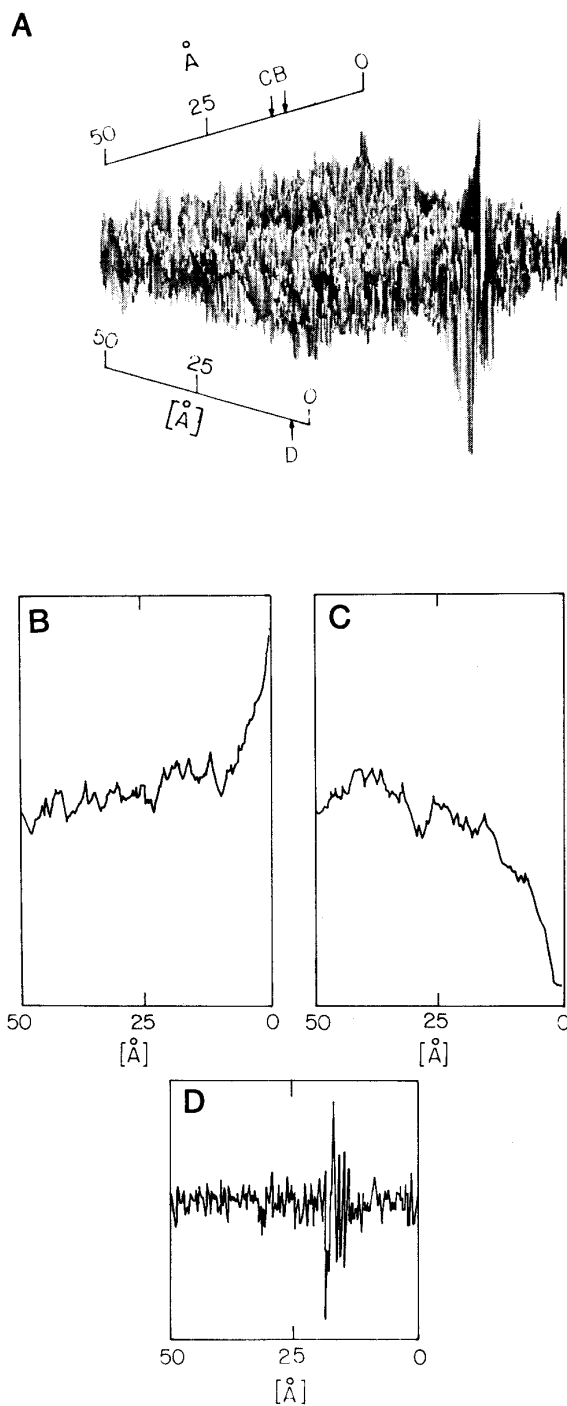


FIG. 4. A two-dimensional ESR-STM spectrum observed with a spectrum analyzer at a constant frequency and a lock-in amplifier. The modulation conditions are described in the text. (B, C) Cross sections that intersect the y axis at the points marked by the arrows. (D) A cross section that intersects the x axis at the point marked by the arrow. A single line scan is approximately three seconds.

tween the unmodulated signal and the detection band of the spectrum analyzer (Fig. 2). The fact that this frequency difference fluctuates creates a random fluctuation of the sign

of the PSD output. One should realize that the STM tip scans the surface line by line. Only after completing a whole line scan in the x direction does the tip scan a parallel line with a slightly different y coordinate. Traces B and C are cross sections parallel to the x axis (the fast scan direction), while trace D is a cross section parallel to the y axis. The frequency fluctuations are slow compared to the time it takes for a single line scan, but fast compared to the rate of changing the y coordinate. As can be seen in trace D, the signal appeared in more than 30 parallel line scans as the tip passes the relevant region (the image is 256×256). This confirms that the signal is spatially localized in two dimensions. The radius of the region from which the signal is induced is in agreement with previous measurements [for example, see Ref. (1)]. Due to the PSD, however, this observation is much more reliable.

To summarize, the real-time response of the ESR-STM signals as detected with and without phase-sensitive detection provides strong experimental proof for the existence of this phenomenon. However, there is a need for a better

understanding of the mechanism, a better S/N ratio of the signal, and a better characterization of the dependence on various experimental parameters before this technique can be exploited.

ACKNOWLEDGMENTS

This work was supported by the Minerva Foundation, Munich, Germany, and the Basic Research Foundation administered by the Israeli Academy of Sciences and Humanities. The author is an incumbent of the Lilian and George Lyttle Career Development Chair.

REFERENCES

1. Y. Manassen, R. J. Hamers, J. E. Demuth, and A. J. Castellano, Jr., *Phys. Rev. Lett.* **62**, 2531 (1989).
2. Y. Manassen, E. Ter-Ovanesyan, D. Shachal, and S. Richter, *Phys. Rev. B* **48**, 4887 (1993).
3. Y. Manassen, E. Ter-Ovanesyan, and D. Shachal, in "Bioradicals Detected with ESR Spectroscopy" (H. Ohya-Nishiguchi and L. Packer, Eds.), Birkhäuser, Basel/Switzerland, 1995.
4. F. E. Terman, "Electronic and Radio Engineering," 4th ed., McGraw-Hill, New York, 1955.